The Astrophysical Journal, 618:601–608, 2005 January 10

THE LARGEST BLUESHIFTS OF THE [O III] EMISSION LINE IN TWO NARROW-LINE QUASARS

Kentaro Aoki[1]
Subaru Telescope, National Astronomical Observatory of Japan, 650 North A'ohoku Place, Hilo, HI 96720; kaoki@naoj.org
Toshihiro Kawaguchi[1,2]
LUTH, Observatoire de Paris, Section de Meudon, 5 Place Jules Janssen, 92195 Meudon, France; kawaguti@optik.mtk.nao.ac.jp
and
Kouji Ohta[1]
Department of Astronomy, Kyoto University, Kyoto 606-8502, Japan; ohta@kusastro.kyoto-u.ac.jp
Received 2004 August 23; accepted 2004 September 22

ABSTRACT

We have obtained optical intermediate-resolution spectra ($R = 3000$) of the narrow-line quasars DMS 0059−0055 and PG 1543+489. The [O III] emission line in DMS 0059−0055 is blueshifted by 880 km s^{-1} relative to Hβ. We also confirm that the [O III] emission line in PG 1543+489 has a relative blueshift of 1150 km s^{-1}. These two narrow-line quasars show the largest [O III] blueshifts known to date among type 1 active galactic nuclei (AGNs). The [O III] emission lines in both objects are broad (1000–2000 km s^{-1}), and those in DMS 0059−0055 show strong blue asymmetry. We interpret the large blueshift and the profile of the [O III] lines as the result of an outflow interacting with circumnuclear gas. Among type 1 AGNs with large blueshifted [O III], there is no correlation between the Eddington ratios and the amount of [O III] blueshift. Combining our new data with published results, we confirm that the Eddington ratios of such AGNs are the highest among AGNs with the same black hole mass. These facts suggest that the Eddington ratio is a necessary condition for [O III] blueshifts or that the [O III] blueshifts weakly depend on the Eddington ratio. Our new sample suggests that there are possibly other necessary conditions to produce an outflow than a high Eddington ratio: a large black hole mass ($>10^7\ M_\odot$), a high mass accretion rate ($>2\ M_\odot$ yr^{-1}), or a large luminosity [$\lambda L_\lambda(5100\ \text{Å}) > 10^{44.6}$ ergs s^{-1}].

Subject headings: galaxies: active — quasars: emission lines — quasars: individual (DMS 0059−0055, PG 1543+489)

1. INTRODUCTION

Narrow-line Seyfert 1 galaxies (NLS1s) are a subclass of active galactic nuclei (AGNs) that have the following characteristics (see Pogge 2000): (1) They have relatively narrower permitted lines (Hβ FWHM $\leq$ 2000 km s^{-1}) than those of "normal" broad-line Seyfert 1 galaxies (BLS1s). The 2000 km s^{-1} FWHM of Hβ is usually used to separate NLS1s and BLS1s. (2) They often emit strong optical Fe II multiplets or higher ionization iron lines, which are seen in Seyfert 1 galaxies but not seen in Seyfert 2 galaxies (Osterbrock & Pogge 1985). (3) Their X-ray spectra are significantly softer (photon indices in soft X-ray are $\Gamma = 1.5-5$) than those of BLS1s ($\Gamma \sim 2.1$) (Boller et al. 1996; Laor et al. 1997). (4) They show rapid soft/hard X-ray variability (Leighly 1999a). The most likely interpretation of these characteristics is that for a given luminosity, NLS1s contain lower mass black holes with higher accretion rates than do BLS1s (Boroson 2002). NLS1s tend to have larger Eddington ratios, which is the ratio of the bolometric to Eddington luminosity, than do BLS1s (e.g., Kawaguchi 2003).

Outflow phenomena have been reported in some NLS1s and narrow-line quasars (NLQs), which are luminous ($M_B < -23$ mag) counterparts of NLS1s. I Zw 1, the prototype of NLS1s/NLQs, has been known to have [O III] $\lambda\lambda$4959, 5007 emission lines blueshifted by 600 km s^{-1} relative to other emission lines (Phillips 1976). The redshift of Hβ in I Zw 1 is consistent with the redshift of the centroid of the H I 21 cm line (Condon et al. 1985) and the molecular CO line (Barvainis et al. 1989), which represent the systemic redshift of the object more reliably. The [O III] emission line in I Zw 1 is thus blueshifted relative to not only Hβ but also the systemic velocity. Zamanov et al. (2002) discovered that six other AGNs show [O III] blueshifts relative to Hβ that are larger than 250 km s^{-1} among a sample of 216 type 1 AGNs. We hereafter refer to them as "blue outliers," following Zamanov et al. (2002). The broad Hβ lines of blue outliers are narrow ($\leq$4000 km s^{-1}), and half of them are NLQs. The large [O III] blueshift is interpreted as the result of an outflow whose receding part is obscured by an optically thick accretion disk (Zamanov et al. 2002). The origin of the outflow is considered to be strong radiation pressure due to a large Eddington ratio (Grupe & Leighly 2002; Zamanov et al. 2002).

Although more than 10 blue outliers have been found (Grupe & Leighly 2002; Zamanov et al. 2002; Marziani et al. 2003b), there are no detailed observations of their [O III] line profiles. Higher resolution data are crucial to identifying their weak [O III] emission lines, which are blended with strong Fe II emission lines. The previous observations were carried out with a resolution of 5–7 Å, i.e., a resolving power of $R = 1000-1500$. Therefore, we have carried out higher resolution spectroscopy ($R = 3000$) of two NLQs, DMS 0059−0055 and PG 1543+48, around the Hβ–[O III] λ5007 region. These two NLQs have the largest known [O III] blueshifts among type 1 AGNs. It is important to observe the objects with the most extreme blueshift in order to understand the [O III] outflow phenomena. If the origin of the outflow is radiation pressure, objects with more

[1] Visiting Astronomer, Kitt Peak National Observatory, National Optical Astronomy Observatory, which is operated by the Association of Universities for Research in Astronomy, Inc. (AURA) under cooperative agreement with the National Science Foundation.
[2] Postdoctoral Fellow of the Japan Society for the Promotion of Science.

luminosity and/or higher Eddington ratios are expected to show larger blueshifts. Marziani et al. (2003b) indeed showed that blue outliers have higher Eddington ratios among AGNs with similar black hole masses.

DMS 0059−0055 ($z = 0.295$) was discovered by the Deep Multicolor CCD Survey (Kennefick et al. 1997). DMS 0059−0055 is included as SDSS J010226.31−003904.6 in the NLS1 sample of Williams et al. (2002). They searched the Sloan Digital Sky Survey (SDSS; York et al. 2000) Early Data Release (EDR; Stoughton et al. 2002) for NLS1s and compiled a sample of 150. The Hβ FWHM of DMS 0059−0055 is 1680 km s^{-1} (Williams et al. 2002). Its spectrum also shows prominent Fe II emission lines. Its soft X-ray spectrum is steep, with a photon index of 3.2 (Williams et al. 2002). These characteristics of DMS 0059−0055 are typical for NLS1s/NLQs.

PG 1543+489 ($z = 0.401$) is a radio-quiet quasar in the Bright Quasar Survey (Schmidt & Green 1983). It shows a narrow Hβ (FWHM = 1600 km s^{-1}) emission and strong Fe II emission (Boroson & Green 1992). Its soft X-ray emission has a steep spectral slope with a photon index of 3.1 (Laor et al. 1997). Therefore, PG 1543+489 also has characteristics typical of NLS1s/NLQs. It has the largest [O III] blueshift (950 km s^{-1}) relative to Hβ among the 280 type 1 AGNs in the sample of Marziani et al. (2003b). The [O III] emission is so weak that the [O III] emission line analyzed by Zamanov et al. (2002) has a large uncertainty. This is the reason why we thought a confirmation with a higher S/N ratio and dispersion was necessary.

Here we report the results for spectroscopy of DMS 0059−0055 and PG 1543+489. In § 2 our KPNO observations and the spectrum of DMS 0059−0055 in the SDSS EDR are described. The emission-line properties are presented in § 3. In § 4 we discuss the correlations between the [O III] blueshift, the Eddington ratio, and the optical luminosity among blue outliers. We also compare the Eddington ratios and black hole masses of AGNs with and without an [O III] blueshift and discuss the possible conditions for producing an [O III] outflow. We give concluding remarks in § 5. We assume $H_0 = 70$ km s^{-1} Mpc^{-1}, $\Omega_m = 0.3$, and $\Omega_\Lambda = 0.7$ throughout this paper.

2. OBSERVATIONS AND DATA REDUCTION

2.1. *KPNO Data*

The spectra of DMS 0059−0055 and PG 1543+489 were obtained with the GoldCam spectrograph of the KPNO 2.1 m telescope on 2002 September 16 (UT) and 2003 June 18 (UT), respectively. The nights were under photometric conditions, and the seeing was $\sim 2''$. We binned the F3KC CCD along the slit direction, so the projected pixel size was $1''.56$ along the slit. Grating No. 56 (600 lines mm^{-1}) was used in the second order, and the sampling was 0.65 Å pixel^{-1}. A slit width of $2''.0$ was used, resulting in a resolution of 2.0 Å measured by night sky lines ($R \sim 3000$). The observed spectral range was 6000–7250 Å, which covers lines from Fe II λ4667 to Fe II λ5534 and from Fe II λ4385 to Fe II λ5018 in the rest-frame spectra of DMS 0059−0055 and PG 1543+489, respectively. The slit position angle was 90°. We obtained 5×1800 and 6×1800 s exposures for DMS 0059−0055 and PG 1543+489, respectively. A spectrophotometric standard star, Wolf 1346 or HD 109995, was observed for flux calibration at the beginning of the night.

The data were reduced using IRAF[3] in the standard manner for CCD data. After subtracting the bias level, each spectrum frame was flat-fielded with the internal quartz lamp frames, and then bad columns and cosmic-ray events were removed. Wavelength calibration of each object frame was performed using the comparison lamp frames. A small wavelength offset was corrected by using night-sky lines. The rms wavelength calibration error is 0.05 Å, and it corresponds to 3 km s^{-1} at 6300 Å, to which Hβ and [O III] are redshifted in these objects. After sky subtraction, flux calibration was performed. The sensitivity along wavelength was calibrated within an uncertainty of 3%–4%. One-dimensional spectra were extracted, and all five and six spectra were combined to one spectrum each for DMS 0059−0055 and PG 1543+489, respectively. The atmospheric *B*-band absorption overlapped with the Fe II λ5317 line of DMS 0059−0055 and the Fe II λ4924 line of PG 1543+495. The absorption feature was removed using the standard star's spectrum. The Galactic interstellar reddening was corrected using $E(B-V) = 0.036$ and 0.018 mag (Schlegel et al. 1998) for DMS 0059−0055 and PG 1543+489, respectively, the empirical selective extinction function by Cardelli et al. (1989), and $R_V \equiv A(V)/E(B-V) = 3.1$.

2.2. *SDSS Data*

The spectrum of DMS 0059−0055 in the SDSS EDR was obtained on 2000 September 29 with the 2.5 m telescope at Apache Point Observatory. The spectral resolution is $\sim$1800, and the wavelength coverage is 3800–9200 Å (Stoughton et al. 2002). The flux and wavelength calibration were done by the spectroscopic pipelines (Stoughton et al. 2002). The interstellar reddening was corrected using $E(B-V) = 0.036$ mag, which is the same value used for the KPNO data.

2.3. Fe II *Subtraction*

Both NLQs show strong Fe II emission lines that must be removed for the measurement of the [O III] emission line. The Fe II emission lines were subtracted by the template method of Boroson & Green (1992). The Fe II template was made from a spectrum of I Zw 1. We observed I Zw 1 with the same configuration as PG 1543+489 and DMS 0059−0055 except for the wavelength coverage (4200–5400 Å). The power-law continuum was determined at 4200 and 4750 Å, at which Fe II contamination is relatively weak. After subtracting the continuum, Hβ, Hγ, [O III] $\lambda\lambda$4959, 5007, and [Fe II] emission lines were fitted and subtracted. Balmer lines were fitted with a Lorentzian plus a Gaussian, and [Fe II] emission lines were fitted with a Lorentzian. The [O III] emission lines of I Zw 1 are known to be broad and cannot be fitted with a single Gaussian (Véron-Cetty et al. 2001). We thus fitted the [O III] $\lambda\lambda$4959, 5007 lines using two sets of two Gaussians. The width and redshift were fixed for each set, and the intensity ratio of [O III] λ5007 to λ4959 was fixed to be 3.0.

The power-law continuum was subtracted from the spectra of PG 1543+489 and DMS 0059−0055 by using the same method applied to I Zw 1. Next, the Fe II template was fitted to and subtracted from the continuum-subtracted spectrum. The Fe II template was fitted by changing scaling and broadening factors within reasonable ranges at the red half of the Fe II λ5018 emission line, for which the contamination of Hβ and [O III] is the smallest.

3. RESULTS

3.1. *DMS 0059−0055*

The rest-frame spectra of DMS 0059−0055 obtained with the KPNO 2.1 m and the SDSS EDR are shown in Figure 1.

[3] IRAF is distributed by the National Optical Astronomy Observatory, which is operated by AURA under cooperative agreement with the National Science Foundation.

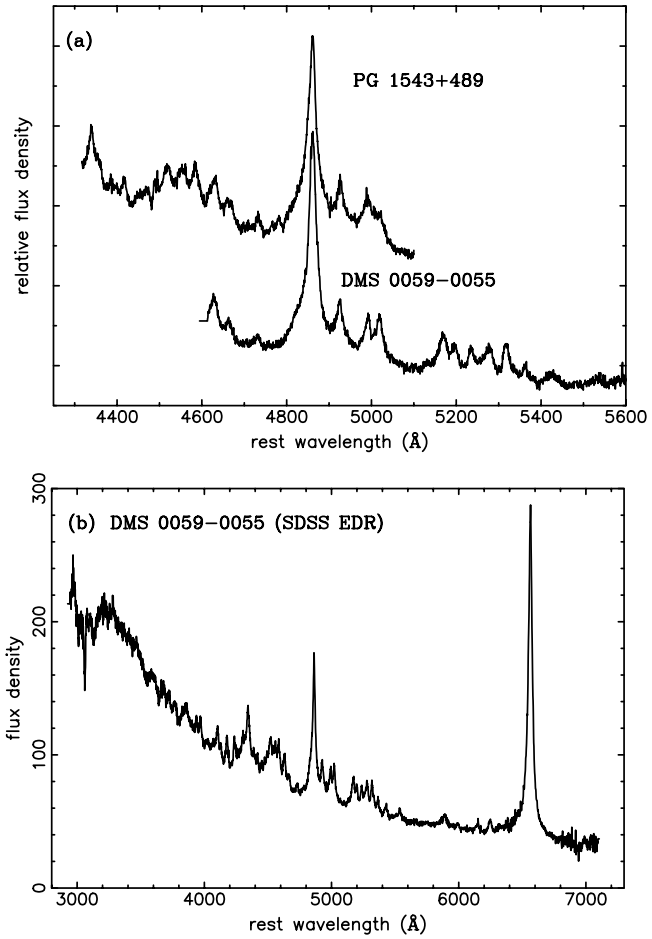

FIG. 1.—Deredshifted spectra of DMS 0059−0055 and PG 1543+489. (*a*) Spectra of DMS 0059−0055 and PG 1543+489 obtained with the KPNO 2.1 m. The ordinate is the relative flux density in units of ergs s^{-1} cm^{-2} $Å^{-1}$, and the abscissa is the rest wavelength in angstroms. The spectra are normalized and shifted by arbitrary values. (*b*) Spectrum of DMS 0059−0055 in the SDSS EDR. The ordinate is the flux density in units of 10^{-17} ergs s^{-1} cm^{-2} $Å^{-1}$, and the abscissa is the rest wavelength in angstroms.

The redshift for Hβ emission was used for the deredshifting. Figure 2 displays the Fe II–subtracted spectrum around the Hβ–[O III] region (*middle spectrum*) obtained with KPNO 2.1 m, as well as the Fe II template (*bottom spectrum*) and the continuum-subtracted spectrum (*top spectrum*) before the Fe II template subtraction. In the middle spectrum there is an emission line whose peak is at 4992.2 ± 1.0 Å, and the width is comparable to those of Fe II and Hβ. If this feature is the blueshifted [O III] λ5007 emission line as found in several NLQs (Zamanov et al. 2002; Marziani et al. 2003b), the corresponding [O III] λ4959 line should be seen at 4944.2 Å with one-third of the flux of the λ4992 feature. The [O III] λ4959 line at first glance does not seem to exist in the Fe II–subtracted spectrum. However, we can obtain an acceptable fit to the spectrum with [O III] $\lambda\lambda$4959, 5007 together with Hβ, as shown in Figure 3. We thus identify the λ4992 feature with the [O III] λ5007 emission line. Since the λ4992 feature has an asymmetric profile (i.e., not well fitted with a single Gaussian), the [O III] $\lambda\lambda$4959, 5007 lines are fitted with two Gaussians for each line. Hβ was fitted with a combination of a Lorentzian and a Gaussian. The FWHMs were corrected for the instrumental broadening using the simple assumption $\mathrm{FWHM_{true}} = (\mathrm{FWHM^2_{obs}} - \mathrm{FWHM^2_{inst}})^{1/2}$, where $\mathrm{FWHM_{obs}}$ is the observed FWHM of a line and $\mathrm{FWHM_{inst}}$ is the instrumental FWHM. The fitting result is shown in Figure 3.

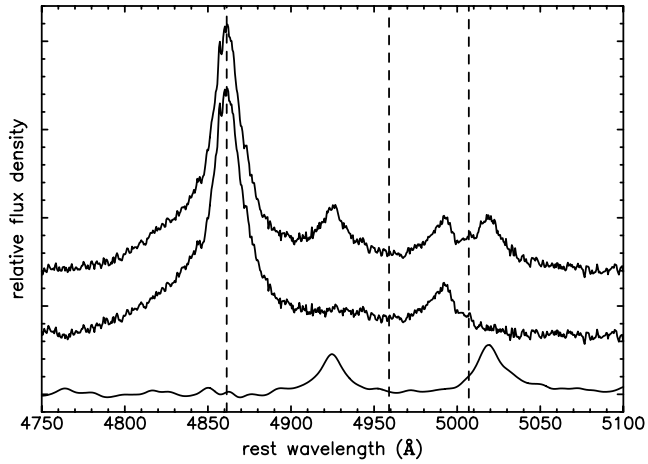

FIG. 2.—Fe II–subtracted spectrum of DMS 0059−0055. The ordinate is the relative flux density in units of ergs s^{-1} cm^{-2} $Å^{-1}$, and the abscissa is the rest wavelength in angstroms. The top plot is the continuum-subtracted spectrum, the middle is the Fe II–subtracted one, and the bottom is the Fe II template used. These three spectra are shifted by adding arbitrary constants. The dashed lines mark the wavelengths of Hβ and [O III] $\lambda\lambda$4959, 5007 expected from the redshift of the Hβ peak.

One [O III] component, with FWHM = 2300 ± 150 km s^{-1}, is blueshifted by 1240 ± 100 km s^{-1} relative to Hβ, and the other component, with FWHM = 580 ± 70 km s^{-1}, is blueshifted by 880 ± 30 km s^{-1}. The broad profile and large blueshift merge [O III] λ4959 into the red wing of the Hβ broad line and smear [O III] λ4959. The large blueshifted [O III] emission line in DMS 0059−0055 has been newly discovered in this work. The [O III] λ5007 profile shows asymmetry and has a strong blue tail. The directly measured FWHM of [O III] λ5007 is 1320 ± 80 km s^{-1}, while that of Hβ is 1500 ± 50 km s^{-1}.

The Fe II–subtracted spectrum from the SDSS EDR is consistent with the KPNO spectrum except for the line width of the narrower component of [O III]. One [O III] component, with FWHM = 2310 ± 130 km s^{-1}, is blueshifted by 1200 ± 80 km s^{-1} (relative to Hβ), and the other component, with FWHM = 840 ± 150 km s^{-1}, is blueshifted by 860 ± 40 km s^{-1}. The spectral resolution of the SDSS EDR spectrum is a factor of ~2

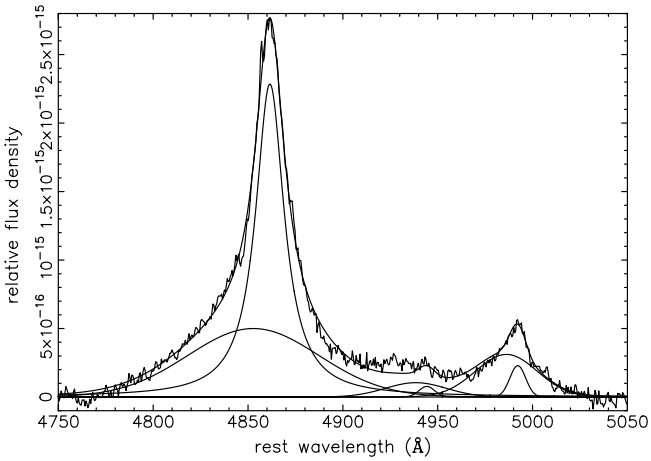

FIG. 3.—Fit of the Hβ–[O III] region of DMS 0059−0055. The ordinate is the relative flux density in units of ergs s^{-1} cm^{-2} $Å^{-1}$, and the abscissa is the rest wavelength in angstroms. Hβ is fitted with a Lorentzian and a Gaussian, and the [O III] doublet is fitted with two sets of two Gaussians. Note that the continuum was subtracted.

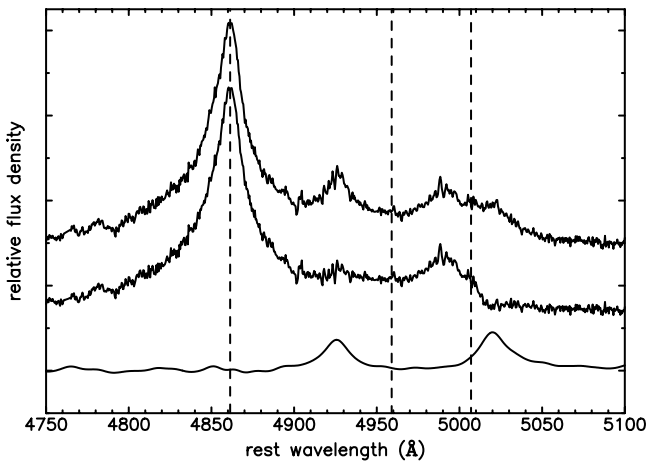

FIG. 4.—Fe II–subtracted spectrum of PG 1543+489. The ordinate is the relative flux density in units of ergs s^{-1} cm^{-2} $Å^{-1}$, and the abscissa is the rest wavelength in angstroms. The top plot is the continuum-subtracted spectrum, the middle is the Fe II–subtracted one, and the bottom is the Fe II template used. These three spectra are shifted by adding arbitrary constants. The dashed lines mark the wavelengths of Hβ and [O III] $\lambda\lambda$4959, 5007 expected from the redshift of the Hβ peak.

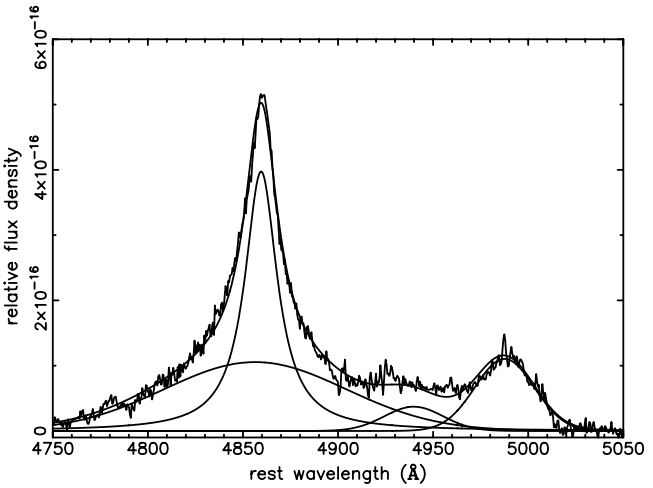

FIG. 5.—Fit of the Hβ–[O III] region of PG 1543+489. The ordinate is the relative flux density in units of ergs s^{-1} cm^{-2} $Å^{-1}$, and the abscissa is the rest wavelength in angstroms. Hβ is fitted with a Lorentzian and a Gaussian, and the [O III] doublet is fitted with a Gaussian. Note that the continuum was subtracted.

lower than that of our KPNO spectrum, while the S/N of the SDSS EDR spectrum is comparable to that of our KPNO spectrum. The line width of the narrower component of [O III] in the SDSS spectrum is significantly broader than that in the KPNO spectrum. Although we could not find any reason for the discrepancy in the line width, we prefer the result from the KPNO spectrum because it was obtained with a higher spectral resolution and a comparable S/N. Since the SDSS spectrum was absolute flux calibrated, we can measure the [O III] flux. The [O III] λ5007 flux is $(1.4 \pm 0.5) \times 10^{-15}$ ergs s^{-1} cm^{-2} for the narrower component and $(5.7 \pm 0.5) \times 10^{-15}$ ergs s^{-1} cm^{-2} for the broader one.

In order to estimate the ratio of [O III] λ5007/Hβ for the [O III]–emitting gas, we tried to fit the spectrum with the components described above plus two Gaussians that represent blueshifted Hβ from the [O III]–emitting gas. The FWHM and redshift were fixed to be the same values as for the corresponding [O III] component. The intensity ratio of the broad component to the narrow one was also fixed to the same value as for the [O III] component. However, the fitting result did not converge. We could not estimate the flux of the blueshifted Hβ corresponding to the [O III] component.

In order to measure the Fe II emission line between 4434 and 4684 Å (hereafter Fe II λ4570), we used the continuum-subtracted SDSS spectrum. The flux of Fe II λ4570 is 4.4×10^{-14} ergs s^{-1} cm^{-2}. Since the flux of Hβ is $(4.3 \pm 1.1) \times 10^{-14}$ ergs s^{-1} cm^{-2}, the flux ratio of Fe II λ4570/Hβ is 1.0. The large Fe II λ4570/Hβ makes DMS 0059−0055 a strong Fe II emitter. This fact is consistent with the indication by Zamanov et al. (2002) that blue outliers tend to show strong Fe II emission.

3.2. *PG 1543+489*

The spectrum of PG 1543+489 deredshifted by referring to the Hβ peak is shown in Figure 1. Figure 4 displays the Fe II–subtracted spectrum around the Hβ–[O III] region (*middle spectrum*) obtained with the KPNO 2.1 m, as well as the Fe II template (*bottom spectrum*) used and the continuum-subtracted spectrum (*top spectrum*) before the Fe II template subtraction. Our spectrum was taken with a spectral resolution 3 times higher than that by Boroson & Green (1992). The fitting result for PG 1543+489 around the Hβ–[O III] region is shown in Figure 5. The spectrum of PG 1543+489 is similar to that of DMS 0059−0055, except for the absence of a blue tail in the [O III] line in PG 1543+489. Hβ was fitted with a Lorentzian plus a Gaussian. The [O III] $\lambda\lambda$4959, 5007 lines were fitted with a broad (FWHM = 2200 ± 40 km s^{-1}), blueshifted (1150 ± 20 km s^{-1} relative to Hβ) Gaussian. This [O III] blueshift is 20% larger than that reported previously (Zamanov et al. 2002; Marziani et al. 2003b). Comparing Figure 2 in Zamanov et al. (2002) and our Figure 5, our spectrum has a higher S/N ratio, as well as a resolution that is 3 times higher. Our blueshift measurement thus seems more reliable, and the disagreement is probably due to improvement of data quality. The directly measured FWHM of Hβ is 1630 ± 50 km s^{-1}, which is consistent with 1600 km s^{-1} (Zamanov et al. 2002) and 1560 km s^{-1} (Boroson & Green 1992; Marziani et al. 2003b). The absolute flux of [O III] could not be measured for PG 1543+489, since the spectroscopy at KPNO was done with a slit width comparable to the seeing size.

As done for DMS 0059−0055, we tried to detect a blueshifted Hβ emission line. Adding a single Gaussian that represented a blueshifted Hβ with the same width and redshift as the [O III] line, we have fitted a spectrum as shown in Figure 6. The [O III] λ5007/Hβ is 0.38. Although the fit converged in this case, this blueshifted Hβ line is completely buried under the blue wing of Hβ. Therefore, we think that the blueshifted Hβ is only marginally detected and that its flux has a large uncertainty.

We measured the flux of Fe II λ4570 from the continuum-subtracted spectrum. The flux ratio of Fe II λ4570 to Hβ is 0.85; it agrees well with that of Boroson & Green (1992) but is 30% larger than that of Zamanov et al. (2002). Although Boroson & Green (1992) and Zamanov et al. (2002) analyzed the same spectrum, their Fe II λ4570/Hβ ratios are different: 0.86 (Boroson & Green 1992) and 0.64 (Zamanov et al. 2002). Considering such a discrepancy in measurements from the same data, our result is consistent with the previous measurements.

4. THE NECESSARY CONDITIONS FOR [O III] OUTFLOWS

The blueshift velocity of [O III] in DMS 0059−0055 (880 km s^{-1}) is comparable to that of PG 1543+489 (1150 km s^{-1}), which has the largest blueshift of [O III] among ~280 type 1

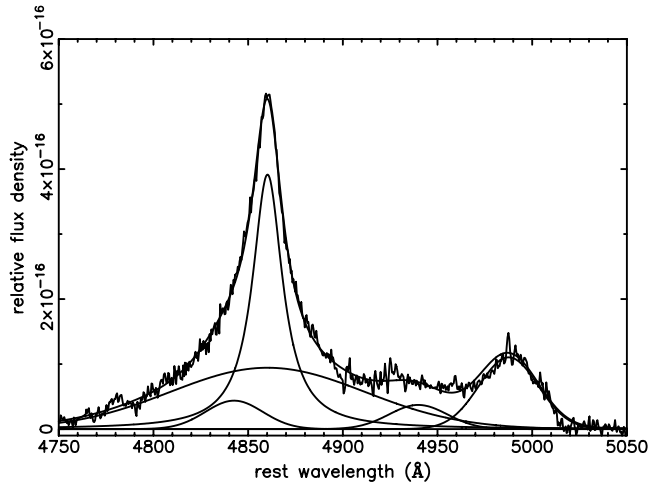

FIG. 6.—Same as Fig. 5, but with an Hβ line added that is blueshifted by the same amount as the [O III] emission.

AGNs (Marziani et al. 2003b). Our spectroscopy reveals that the [O III] lines in both DMS 0059−0055 and PG 1543+489 are broad (1000–2000 km s^{-1}). In particular, a strong blue tail is prominent in the [O III] line of DMS 0059−0055. The [O III] blueshift relative to Hβ together with the strong blue tail suggest that the [O III] is emitted from outflowing gas from the nucleus and that the receding part of the flow is obscured (Zamanov et al. 2002). The large width suggests that the outflow interacts with the surrounding gas. Although it is difficult to reject completely the possibility that optically thick gas is inflowing toward the black hole and the inflowing gas at the near side of the black hole is not seen, we prefer the outflow hypothesis. If the inflowing gas is Thomson thick ($>10^{24}$ cm^{-2}), the redshifted absorption line should be observed in some blue outliers. If the inflowing gas is dusty and optically thick, nuclear broad lines and a continuum may be significantly reddened. However, neither phenomenon is observed in blue outliers.

Since DMS 0059−0055 and PG 1543+489 have the largest [O III] blueshifts known, we would expect them to have extreme characteristics among blue outliers. These extreme objects would enable us to understand the origin of the [O III] outflow. In order to search for a clue to the origin of the [O III] outflow, we compiled blue outliers from the literature and examined correlations between the velocity shift of [O III] relative to Hβ (hereafter referred to as Δv) and several other properties (the Eddington ratio, the optical luminosity, etc.). Marziani et al. (2003b) measured Δv among the type 1 AGN samples of Marziani et al. (2003a), which contain 215 $z \lesssim 0.8$ AGNs, and of Grupe et al. (1999), which is a soft X-ray–selected sample. They found 12 objects with $\Delta v < -250$ km s^{-1} and identified them as blue outliers. Since Zamanov et al. (2002) found that all blue outliers have an Hβ FWHM $\lesssim 4000$ km s^{-1}, we looked for blue outliers among NLS1s/NLQs in Véron-Cetty et al. (2001) and Leighly (1999b). We do not think that Zamanov et al. (2002) missed blue outliers in BLS1s/QSOs because it is easier to measure the [O III] emission line in BLS1s/QSOs than in NLS1s/NLQs; BLS1s/QSOs have stronger [O III] emission and weaker Fe II emission, which contaminates [O III] emission, than do NLS1s/NLQs. We have found that IRAS 04416+1215 and IRAS 04576+0912 have $\Delta v < -250$ km s^{-1} from Figure 1 of Véron-Cetty et al. (2001). Grupe & Leighly (2002) reported that IRAS 13224−3809 has $\Delta v = -370$ km s^{-1}. In the end, we compiled a list of 16 blue outliers including DMS 0059−0055 from our new data. We tabulated the Δv, FWHM of [O III] λ5007, FWHM of Hβ, and their references for the 16 blue outliers in Table 1 in order of Δv.

The optical luminosity λL_λ(5100 Å) of the blue outliers was estimated from the B magnitude given in Véron-Cetty & Véron (2003) and the Galactic extinction A_B, which is calculated from the $E(B-V)$ values of Schlegel et al. (1998) and given in the NED.[4] The k-correction was done by assuming $f_\nu \propto \nu^{-0.44}$

[4] The NASA/IPAC Extragalactic Database (NED) is operated by the Jet Propulsion Laboratory, California Institute of Technology, under contract with the National Aeronautics and Space Administration.

TABLE 1
BLUE OUTLIERS

Name	Δv (km s^{-1})	FWHM [O III] (km s^{-1})	FWHM Hβ (km s^{-1})	Reference	$\log \lambda L_{5100}$ (ergs s^{-1})	$\log M_{\rm BH}$ ($M_\odot$)	$\log \frac{L_{\rm bol}}{L_{\rm Edd}}$	$\log P$ (W Hz^{-1})	$\log R$
PG 1402+261	−300	900	1940	3	45.19	8.09	0.10	22.69	−0.67
IRAS 04416+1215	−300[a]	1320	1470	4	45.11	7.79	0.32	23.18	−0.072
IRAS 04576+0912	−300[a]	1290	1210	4	43.68	6.62	0.06	...	...
PG 0804+761	−305	780	3300	3	44.97	8.40	−0.42	22.80	−0.33
RX J2217.9−5941	−330[b]	1140	1370	3	44.92	7.59	0.32	...	...
IRAS 13224−3809	−370[c]	810	>650[d]	1, 2	45.14	7.10	1.04	22.58	−0.70
RX J0136.9−3510	−380	900	1050	3	44.73	7.24	0.50	...	...
MS 2340.9−1511	−420	780	970	3	44.50	7.01	0.50	<22.68	<0.0070
PKS 0736+01	−430	720	3260	3	44.98	8.39	−0.41	26.23	3.1
RX J2340.6−5329	−490	780	1230	3	44.99	7.55	0.44	...	...
RX J0439.7−4540	−580	1020	1020	3	45.04	7.43	0.62	...	...
PG 1415+451	−600	660	2560	3	44.96	8.17	−0.21	22.15	−0.97
I Zw 1	−640	1440	1090	3	44.83	7.34	0.49	22.38	−0.59
Ton 28	−680	960	1760	3	45.60	8.29	0.31	...	...
DMS 0059−0055	−880	1320	1500	5	45.28	7.93	0.35	...	...
PG 1543+489	−1150	2200	1630	5	45.59	8.05	0.37	23.86	0.0054

[a] These values were measured by us from the figure in Véron-Cetty et al. (2001).
[b] This is −570 km s^{-1} in Grupe et al. (2001).
[c] This value was measured by us from the figure in Grupe & Leighly (2002).
[d] The Hβ seems to be contaminated by an H II region. This value may be a lower limit (K. Leighly 2004, private communication).
REFERENCES.—(1) Grupe & Leighly 2002; (2) Leighly 1999b; (3) Marziani et al. 2003b; (4) Véron-Cetty et al. 2001; (5) this study.

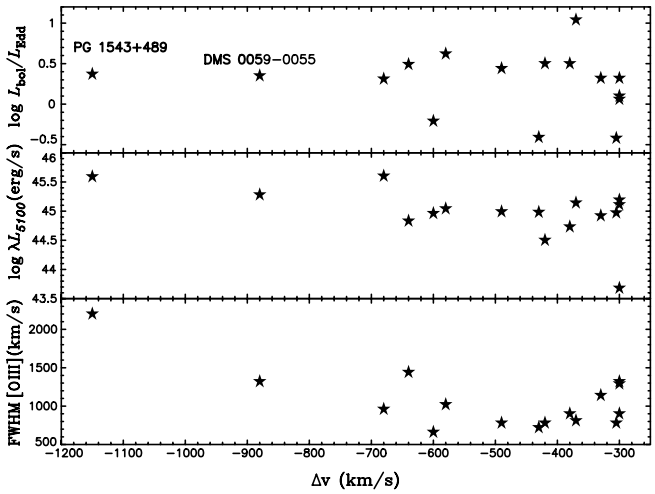

FIG. 7.—Blueshift velocity (Δv) vs. the Eddington ratio (*top*), the optical luminosity (*middle*), and the [O III] line width (*bottom*). No properties significantly correlate with Δv.

(Vanden Berk et al. 2001). The Eddington ratio was calculated from the Eddington luminosity, $1.3 \times 10^{38} M_{\rm BH}/M_\odot$ ergs s^{-1}, and the bolometric luminosity $L_{\rm bol}$, which is assumed to be $13\lambda L_\lambda(5100\ \text{Å})$ ergs s^{-1} (Elvis et al. 1994). The black hole mass $M_{\rm BH}$ was estimated using the relation between size of the broad-line region and the luminosity and the assumption of virialized motions in broad-line regions (Kaspi et al. 2000) as

$$M_{\rm BH} = 4.817 \times 10^6 \left[\frac{\rm FWHM(H\beta)}{10^3\ \rm km\ s^{-1}}\right]^2 \left[\frac{\lambda L_\lambda(5100\ \text{Å})}{10^{44}\ \rm ergs\ s^{-1}}\right]^{0.7} M_\odot.$$

Note that most of the NLS1s/NLQs in Kaspi et al. (2000) also follow the same relation as do BLS1s/QSOs. Therefore, black hole mass estimation with Hβ width and optical luminosity (Wandel et al. 1999; Kaspi et al. 2000) is likely to be valid not only for BLS1s/QSOs but also for NLS1s/NLQs. We simply assume (as is done by Marziani et al. [2003b]) that this black hole mass estimation can also work for blue outliers, although the relation between the size of the broad-line region and the luminosity for blue outliers has not been obtained observationally. The lack of apparent difference in Hβ profiles between blue outliers and other NLS1s/NLQs without [O III] outflows supports this assumption.

We also examine their radio properties; we took radio flux data from the literature for nine blue outliers and calculated the monochromatic radio luminosity at 5 GHz and the radio loudness parameter, $\log R$. Here R is the ratio of radio (5 GHz) to optical (B band) flux density. Table 1 also gives $\lambda L_\lambda(5100\ \text{Å})$, $M_{\rm BH}$, the Eddington ratio, the radio luminosity, and the radio loudness parameter.

Figure 7 shows the Eddington ratio, optical luminosity, and [O III] line width versus Δv. No clear correlation is seen between the Eddington ratio and Δv (Fig. 7, *top*); rather, the ratio is roughly constant for various Δv values. The optical luminosity (Fig. 7, *middle*) and the [O III] line width (Fig. 7, *bottom*) seem to correlate with Δv; large Δv tends to occur with large luminosity and large [O III] width. However, the Spearman rank correlation coefficients, $r_{\rm S}$, and their probabilities from null correlation, P_r, for these distributions show no significant correlation (Table 2). Since neither the Eddington ratio nor the optical luminosity correlates with Δv, there is no strong luminosity dependence on Δv among blue outliers. We suspect that the lack of any strong correlations with Δv may indicate that the

TABLE 2
SPEARMAN'S RANK CORRELATION COEFFICIENTS

Property	Type	Δv	FWHM [O III]
Δv	$r_{\rm S}$	...	−0.18
	P_r	...	0.50
$\log L_{\rm bol}/L_{\rm Edd}$	$r_{\rm S}$	−0.24	0.25
	P_r	0.37	0.35
$\log \lambda L_{5100}$	$r_{\rm S}$	−0.37	0.23
	P_r	0.16	0.39
$\log M_{\rm BH}$	$r_{\rm S}$	−0.25	−0.17
	P_r	0.34	0.53
$\log P$	$r_{\rm S}$	0.24	0.18
	P_r	0.57	0.64
$\log R$	$r_{\rm S}$	−0.11	0.075
	P_r	0.80	0.85

Δv is affected by the viewing angle (Marziani et al. 2003b). This may also explain the distribution of data points in Figure 7 (*middle*); as optical luminosity increases, the absolute value of the maximum blueshift among blue outliers at a given luminosity also increases. The maximum blueshift may occur at the smallest viewing angle. The Δv does not depend on the radio properties; neither the radio power nor radio loudness correlates with Δv.

Although Marziani et al. (2003b) pointed out that blue outliers have the highest Eddington ratios among their sample, we could not find any significant correlation between Δv and the Eddington ratio among blue outliers. Moreover, we have found that a number of NLS1s/NLQs in Véron-Cetty et al. (2001) and Leighly (1999b) with high Eddington ratios are not blue outliers. In order to search for other possible conditions necessary for a large [O III] outflow besides a high Eddington ratio, we plotted our blue outlier sample and NLS1s/NLQs in Véron-Cetty et al. (2001) and Leighly (1999b), as well as the Marziani et al. (2003b) sample, in the $M_{\rm BH}$ versus Eddington ratio plane (Fig. 8). The $M_{\rm BH}$ and Eddington ratio of this sample were calculated in the same manner as for our blue outlier sample. While we found that there are no correlations between Δv and the

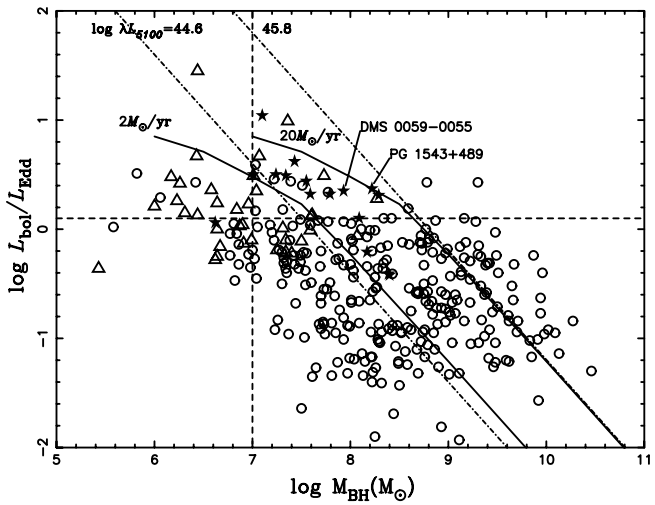

FIG. 8.—Black hole mass vs. Eddington ratio. NLS1s from Véron-Cetty et al. (2001) and Leighly (1999b) are coded as triangles, blue outliers as stars, and type 1 AGNs from Marziani et al. (2003b) as circles. The dashed lines indicate $\log(L_{\rm bol}/L_{\rm Edd}) = 0.1$ and $M_{\rm BH} = 10^7\ M_\odot$, respectively. The solid lines show the Eddington ratio for various $M_{\rm BH}$ with a given M. The dot-dashed lines represent the constant optical luminosity.

Eddington ratio among blue outliers, we confirmed that the blue outliers tend to have higher Eddington ratios than AGNs without [O III] outflows. This fact suggests that either a high Eddington ratio is a necessary condition or that the dependence of Δv on the Eddington ratio is weak and may be affected by viewing angle.

Inspecting Figure 8 prompts us to consider $M_{\rm BH}$ in addition to the Eddington ratio as a factor in the production of the [O III] outflow. The Marziani et al. (2003b) sample includes only a few objects with a small black hole mass ($<10^7\ M_\odot$) and a high Eddington ratio. Our sample includes more such objects. A considerable number of objects with $M_{\rm BH} < 10^7\ M_\odot$ also have high Eddington ratios ($\log L_{\rm bol}/L_{\rm Edd} \geq 0.1$). None of these 15 objects is, however, a blue outlier. On the other hand, there are a dozen blue outliers among the 33 objects with $M_{\rm BH} \geq 10^7\ M_\odot$ and high Eddington ratios. Thus, it seems that $\sim 10^7\ M_\odot$ is the lower limit of $M_{\rm BH}$ for producing an [O III] outflow.

The high Eddington ratio and the large $M_{\rm BH}$ seem to be the conditions necessary for an [O III] outflow. The distribution of blue outliers in Figure 8, however, hints at the presence of another condition. There is a continuous distribution of blue outliers from ($\log M_{\rm BH}$, $\log L_{\rm bol}/L_{\rm Edd}$) = (7, 0.5) to (8.4, −0.4) in Figure 8. This distribution implies that there is a possible lower limit in the mass accretion rate ($\dot{M}$) or the optical luminosity for producing an [O III] outflow. The Eddington ratio decreases with increasing $M_{\rm BH}$ at a constant $\dot{M}$. We show the Eddington ratio for various $M_{\rm BH}$ at a given $\dot{M}$ in Figure 8 (*solid lines*). Bolometric luminosity is computed with the accretion disk model by Kawaguchi (2003), which is applicable to both sub-Eddington and super-Eddington ($\dot{M} \gg L_{\rm Edd}/c^2$) accretion rates. The Eddington ratio is inversely proportional to $M_{\rm BH}$ in the high-$M_{\rm BH}$ range (sub-Eddington accretion rate regime), resulting from a constant bolometric luminosity for a given $\dot{M}$ (i.e., constant radiative efficiency). The bolometric luminosity saturates at a few times Eddington luminosity in the low-$M_{\rm BH}$ range (super-Eddington accretion rate regime), because an accretion disk becomes radiatively inefficient as $\dot{M}/(L_{\rm Edd}/c^2)$ increases (Abramowicz et al. 1988). All blue outliers but one (IRAS 04576+0912)[5] are at the right-hand side of the left solid line in Figure 8, which indicates $\dot{M} \sim 2\ M_\odot\ {\rm yr}^{-1}$. Thus, $\dot{M} \sim 2\ M_\odot\ {\rm yr}^{-1}$ seems to be the lower limit on the mass accretion rate necessary for producing a large [O III] outflow.

The slopes of the lines representing constant $\dot{M}$ and constant optical luminosity on the $M_{\rm BH}$ versus Eddington ratio plane are so similar that it is difficult to distinguish how these two variables affect the presence of blue outliers. The Eddington ratio also decreases when $M_{\rm BH}$ increases at a constant optical luminosity, since the Eddington ratio is expressed as

$$\log\left(\frac{L_{\rm bol}}{L_{\rm Edd}}\right) = -\log\left(\frac{M_{\rm BH}}{10^7 M_\odot}\right) + \log\left[\frac{\lambda L_\lambda\,(5100\ {\rm \AA})}{10^{44}\ {\rm ergs\ s^{-1}}}\right].$$

The dot-dashed lines represent constant optical luminosities in Figure 8. Most blue outliers are located at the right-hand side of the constant $\log[\lambda L_\lambda(5100\ {\rm \AA})/({\rm ergs\ s^{-1}})] = 44.6$, indicating that $\log[\lambda L_\lambda(5100\ {\rm \AA})/({\rm ergs\ s^{-1}})] \gtrsim 44.6$ is also necessary for a large [O III] outflow. We conclude that not only the Eddington ratio but also $M_{\rm BH}$, $\dot{M}$, or the luminosity may control the [O III] outflow. However, other factors (e.g., viewing angle) may govern Δv, because among blue outliers there is no correlation between Δv and the Eddington ratio or the optical luminosity. Finally, we note that there may be upper limits to $\dot{M}$ or the optical luminosity for producing [O III] outflows. We plotted the lines that correspond to $\dot{M} = 20\ M_\odot\ {\rm yr}^{-1}$ and $\log[\lambda L_\lambda(5100\ {\rm \AA})/({\rm ergs\ s^{-1}})] = 45.8$ in Figure 8. The small number of objects with high Eddington ratios whose $\dot{M}$ or luminosity are larger than these lines suggests that these are not strong constraints.

[5] The *B* magnitude, 16.58, of IRAS 04576+0912 may be incorrect. The *J* and K_s magnitudes are 13.8 and 11.9, respectively, from the 2MASS Point Source Catalog. After Galactic reddening correction, $B - K_s = 4.1$ mag, while $J - K_s = 1.9$ mag. $B - K_s$ should be ∼3 mag from $J - K_s$ at $z = 0.037$, adopting the mean QSO spectrum by Elvis et al. (1994). If the luminosity increases by 1 mag, the black hole mass also increases by 0.28 dex. Therefore, the data point moves +0.12 dex along the *y*-axis and +0.28 dex along the *x*-axis in Fig. 8 and is much closer to the line.

5. CONCLUSION

We have obtained optical spectra of the narrow-line quasars DMS 0059−0055 and PG 1543+489 with an intermediate resolution ($R = 3000$). We discovered that DMS 0059−0055 has a large [O III] blueshift relative to Hβ (880 km s^{-1}) and confirmed a large [O III] blueshift in PG 1543+489. The [O III] emission lines in both objects have ∼1000 km s^{-1} blueshifts relative to Hβ, and their widths are more than 1000–2000 km s^{-1}. These large blueshifts and line widths suggest that the outflows occur in their nuclei and interact with the ambient gas.

We examined the correlations between Δv and the Eddington ratio, as well as optical luminosity, among blue outliers, including DMS 0059−0055 and other newly recognized blue outliers. There are no significant correlations of Δv with the Eddington ratio and optical luminosity, contrary to naive expectations based on a radiative pressure–driven outflow hypothesis. However, when we compared the Eddington ratio of blue outliers with those of other type 1 AGNs, we confirmed that blue outliers have the highest Eddington ratio among objects with the same $M_{\rm BH}$. These facts suggest that a high Eddington ratio is a necessary condition, or that Δv depends weakly on the Eddington ratio and the viewing angle may affect Δv. In addition, we found that besides a high Eddington ratio, a higher $M_{\rm BH}$ ($>10^7\ M_\odot$) and a higher mass accretion rate ($>2\ M_\odot\ {\rm yr}^{-1}$) or larger luminosity ($\lambda L_\lambda(5100\ {\rm \AA}) > 10^{44.6}$ ergs s^{-1}) also seem to be necessary to produce an outflow.

We are grateful to the staffs of KPNO for their assistance during our observations. We are also grateful to Anabela Gonçalves, Monique Joly, and Suzy Collin for useful discussions and comments and to Catherine Ishida for improving the manuscript. T. K. is supported by a Japan Society for the Promotion of Science Postdoctoral Fellowship for Research Abroad (464). This research has made use of the NASA/IPAC Extragalactic Database, which is operated by the Jet Propulsion Laboratory, California Institute of Technology, under contract with the National Aeronautics and Space Administration. Funding for the creation and distribution of the SDSS Archive has been provided by the Alfred P. Sloan Foundation, the Participating Institutions, the National Aeronautics and Space Administration, the National Science Foundation, the US Department of Energy, the Japanese Monbukagakusho, and the Max Planck Society. The SDSS Web site is at http://www. sdss.org. The SDSS is managed by the Astrophysical Research Consortium for the Participating Institutions. The Participating Institutions are the University of Chicago, Fermilab, the Institute for Advanced Study, the Japan Participation Group, Johns Hopkins University, Los Alamos National Laboratory, the Max Planck Institute for Astronomy, the Max Planck Institute for Astrophysics, New Mexico State University, the University of Pittsburgh, Princeton University, the United States Naval Observatory, and the University of Washington.

REFERENCES

Abramowicz, M. A., Czerny, B., Lasota, J. P., & Szuszkiewicz, E. 1988, ApJ, 332, 646
Barvainis, R., Alloin, D., & Antonucci, R. 1989, ApJ, 337, L69
Boller, T., Brandt, W. N., & Fink, H. 1996, A&A, 305, 53
Boroson, T. A. 2002, ApJ, 565, 78
Boroson, T. A., & Green, R. F. 1992, ApJS, 80, 109
Cardelli, J. A., Clayton, G. C., & Mathis, J. S. 1989, ApJ, 345, 245
Condon, J. J., Hutchings, J. B., & Gower, A. C. 1985, AJ, 90, 1642
Elvis, M., et al. 1994, ApJS, 95, 1
Grupe, D., Beuermann, K., Mannheim, K., & Thomas, H.-C. 1999, A&A, 350, 805
Grupe, D., & Leighly, K. M. 2002, in X-Ray Spectroscopy of AGN with *Chandra* and *XMM-Newton*, ed. T. Boller (MPE Rep. 279; Garching: MPE), 287
Grupe, D., Thomas, H.-C., & Leighly, K. M. 2001, A&A, 369, 450
Kaspi, S., Smith, P. S., Netzer, H., Maoz, D., Jannuzi, B. T., & Giveon, U. 2000, ApJ, 533, 631
Kawaguchi, T. 2003, ApJ, 593, 69
Kennefick, J. D., Osmer, P. S., Hall, P. B., & Green, R. F. 1997, AJ, 114, 2269
Laor, A., Fiore, F., Elvis, M., Wilkes, B. J., & McDowell, J. C. 1997, ApJ, 477, 93
Leighly, K. M. 1999a, ApJS, 125, 297
———. 1999b, ApJS, 125, 317
Marziani, P., Sulentic, J. W., Zamanov, R., Calvani, M., Dultzin-Hacyan, D., Bachev, R., & Zwitter, T. 2003a, ApJS, 145, 199
Marziani, P., Zamanov, R. K., Sulentic, J. W., & Calvani, M. 2003b, MNRAS, 345, 1133
Osterbrock, D. E., & Pogge, R. W. 1985, ApJ, 297, 166
Phillips, M. M. 1976, ApJ, 208, 37
Pogge, R. W. 2000, NewA Rev., 44, 381
Schlegel, D. J., Finkbeiner, D. P., & Davis, M. 1998, ApJ, 500, 525
Schmidt, M., & Green, R. F. 1983, ApJ, 269, 352
Stoughton, C., et al. 2002, AJ, 123, 485
Vanden Berk, D. E., et al. 2001, AJ, 122, 549
Véron-Cetty, M.-P., & Véron, P. 2003, A&A, 412, 399
Véron-Cetty, M.-P., Véron, P., & Gonçalves, A. C. 2001, A&A, 372, 730
Wandel, A., Peterson, B. M., & Malkan, M. A. 1999, ApJ, 526, 579
Williams, R. J., Pogge, R. W., & Mathur, S. 2002, AJ, 124, 3042
York, D. G., et al. 2000, AJ, 120, 1579
Zamanov, R., Marziani, P., Sulentic, J. W., Calvani, M., Dultzin-Hacyan, D., & Bachev, R. 2002, ApJ, 576, L9